August 1999 • NREL/SR-520-26930

Subcontractor Report

CIS-Type PV Device Fabrication by Novel Techniques

Phase I Annual Technical Report July 1, 1998 – June 30, 1999

B.M. Basol, V.K. Kapur, C.R. Leidholm, A. Halani, G. Norsworthy, and R. Roe
International Solar Electric Technology, Inc.
Inglewood, California

National Renewable Energy Laboratory

1617 Cole Boulevard
Golden, Colorado 80401-3393

NREL is a U.S. Department of Energy Laboratory
Operated by Midwest Research Institute • Battelle • Bechtel

Contract No. DE-AC36-98-GO10337

August 1999 • NREL/SR-520-26930

CIS-Type PV Device Fabrication by Novel Techniques

Phase I Annual Technical Report July 1, 1998 – June 30, 1999

B.M. Basol, V.K. Kapur, C.R. Leidholm, A. Halani, G. Norsworthy, and R. Roe
International Solar Electric Technology, Inc.
Inglewood, California

NREL Technical Monitor: H.S. Ullal

Prepared under Subcontract No. ZAK-8-17619-10

National Renewable Energy Laboratory

1617 Cole Boulevard
Golden, Colorado 80401-3393

NREL is a U.S. Department of Energy Laboratory
Operated by Midwest Research Institute • Battelle • Bechtel

Contract No. DE-AC36-98-GO10337

NOTICE

Available to DOE and DOE contractors from:
Office of Scientific and Technical Information (OSTI)
P.O. Box 62
Oak Ridge, TN 37831
Prices available by calling 423-576-8401

Available to the public from:
National Technical Information Service (NTIS)
U.S. Department of Commerce
5285 Port Royal Road
Springfield, VA 22161
703-605-6000 or 800-553-6847
or
DOE Information Bridge
http://www.doe.gov/bridge/home.html

 Printed on paper containing at least 50% wastepaper, including 20% postconsumer waste

Table of Contents

List of Figures

List of Tables

1.0 Summary

This is the Phase I Annual Technical Progress Report of the R&D partnership subcontract titled "CIS-type PV Device Fabrication by Novel Techniques". The objective of this program is to bring ISET's novel non-vacuum CIS technology closer to commercialization by concentrating on issues such as device efficiency improvement, larger bandgap absorber growth and module fabrication.

Advances made in CIS and related compound solar cell fabrication processes have clearly shown that these materials and device structures can yield power conversion efficiencies in the 15-20% range. However, many of the laboratory results on CIS-type devices have been obtained using relatively high cost vacuum-based deposition techniques. The present project was specifically geared towards the development of a low cost, non-vacuum "particle deposition" method for CIS-type absorber growth. There are four major processing steps in this technique: i) the preparation of a starting powder containing all or some of the chemical species constituting CIS, ii) preparation of an ink using the starting powder, iii) deposition of the ink on a substrate in the form of a thin precursor layer, and iv) conversion of the precursor layer into a fused photovoltaic absorber through annealing steps.

During this Phase I program ISET worked on tasks which were geared towards the following goals: i) elimination of back contact problems, ii) growth of large bandgap absorbers, and iii) fabrication of mini-modules.

As a result of the Phase I research, a Mo back contact structure was developed which eliminated problems that resulted in poor mechanical integrity of the absorber layers. Sulfur inclusion into CIS films through high temperature sulfurization in H_2S gas was also studied. It was determined that S diffusion was a strong function of the stoichiometry of the CIS layer. Sulfur was found to diffuse rapidly through the Cu-rich films, whereas the diffusion constant was at least three orders of magnitude smaller in Cu-poor layers. Additionally, S profiles in sulfurized CIS films were correlated with the distribution of the grain size through the film. Absorbers containing large concentrations of Ga near the Mo contact interface had also large S content in that same region due to the small grain size of the Ga-containing material. New work on monolithic integration procedures overcame the problem of low shunt resistance and yielded $CuIn(S,Se)_2$ (CISS) mini-modules of about 64 cm^2 area with close to 7 % efficiency.

Future work will concentrate on the mini-module efficiency and yield improvement, module stability studies, elimination of the CdS buffer layer and determination of S diffusion mechanisms in Cu-rich and Cu-poor CIS absorbers.

2.0 Introduction

This is the Phase I Annual Technical Progress Report of the R&D partnership subcontract titled "CIS-type PV Device Fabrication by Novel Techniques". The objective of this program is to bring ISET's novel non-vacuum CIS technology closer to commercialization by concentrating on issues such as device efficiency improvement, larger bandgap absorber growth and module fabrication.

Advances made in CIS and related compound solar cell fabrication processes have clearly shown that these materials and device structures can yield power conversion efficiencies in the 15-20% range. However, many of the impressive laboratory results on CIS devices have been obtained using relatively high cost vacuum-based deposition techniques. The present project is specifically geared towards the development of a low cost, non-vacuum "particle deposition" method for CIS-type absorber growth.

2.1 ISET's non-vacuum "particle deposition" technique

Since early 1980's, when the potential of thin film CIS as a PV material was recognized, there has been several attempts to grow solar-cell-quality CIS type absorbers using some of the well known low cost, large area thin film deposition methods such as screen printing and spraying. Although such techniques have been successfully used for the deposition of high quality CdTe absorbers, their utilization for chalcopyrite film growth for PV applications did not bear fruit until recently.

Composition control, or the control of the Cu/(In+Ga) molar ratio is an important concern in chalcopyrite film growth, especially when the deposition has to be carried out on large area substrates. The techniques that are based on particle deposition address this concern by fixing the Cu/(In+Ga) ratio in a source material which contains sub-micron size particles. When the source material is delivered on a large area substrate, forming a precursor layer composed of the small particles, the overall composition of the source material is directly transferred onto the substrate irrespective of thickness non-uniformities which may result from the specific deposition method employed. The general steps of a particle deposition technique as applied to the growth of a CIS absorber layer are listed in Figure 1.

The first step in the technique of Figure 1 is the preparation of a starting powder containing all or some of the chemical species constituting CIS. This starting material can be a mixture of Cu and In powders, a powder containing Cu-In alloys, a mixture of Cu-Se and In-Se species, a powder of CIS, etc. It may further contain Se particles. The second step of the process is to prepare a source material using the starting powder. Typically, liquid media is added to the starting powder at this stage and the particle size is reduced (if needed) through mechanical milling to form a paste or an ink which is suitable for deposition on a substrate in the form of a thin precursor layer.

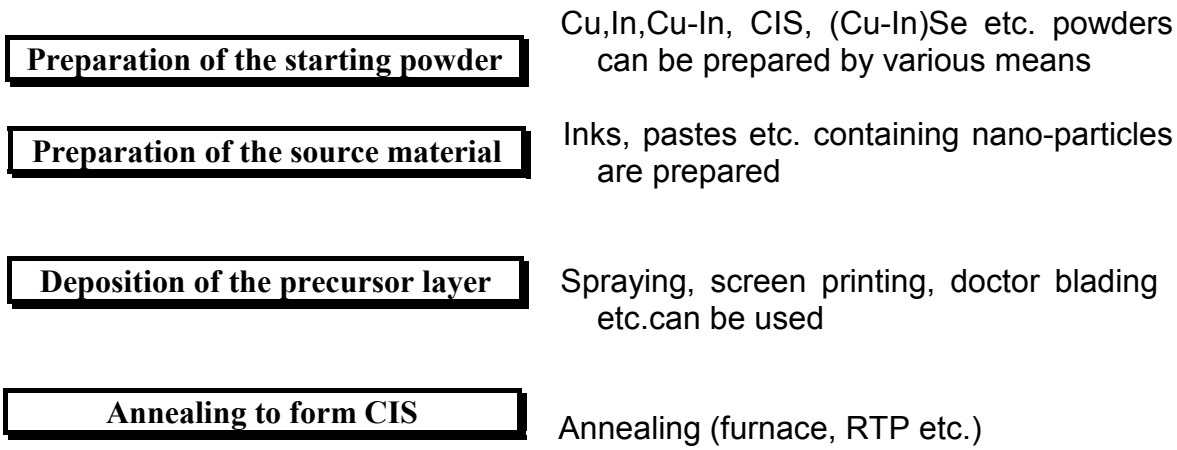

Figure 1 General steps of a CIS growth technique based on particle deposition.

Since the typical thickness of the precursor layer is in the 1-5 μm range, the particle size in the source material should be substantially smaller than 1 μm. In the third step of the process, the source material is coated on the substrate in the form of a precursor layer using low cost techniques such as spraying, screen-printing and doctor blading, among others. The last step involves some form of heat treatment, often in the presence of Se atmosphere. The goal is to form a well-fused and dense compound layer with the fixed Cu/In ratio of the starting powder.

Prior work on particle deposition methods concentrated on screen-printing. The Matsushita group in Japan, for example, mixed pure Cu, In and Se powders and milled this starting powder mixture in liquid media to form a source material in the form of a screen printable paste. Analysis of the paste showed the existence of CIS phase which apparently formed during the ball milling process through the reaction of Cu, In and Se powders. The paste was coated onto substrates and annealed at high temperatures for film fusing. However, the process did not yield solar-cell-quality CIS absorber layers. Researchers at the University of Gent in Europe experimented with various screen printable paste compositions that contained starting powders of CIS rather than a mixture of the elements. Although film sintering and grain growth were observed under certain conditions, the films obtained after the high temperature post-deposition annealing step could not be used for high efficiency solar cell fabrication. The same group also attempted to formulate a paste using the mixture of Cu and In powders without much success.

The prior work reviewed above typically employed starting powders with relatively large particle sizes. These powders were then subjected to mechanical milling with the goal of forming a good quality paste or ink containing sub-micron size particles. Mechanical milling can be effective in reducing the particle sizes of brittle materials such as Cu-Se, In-Se and CIS. However, in approaches employing In powders, for example, the particle size can not

be reduced by standard milling since the soft material would tend to coat the milling media as well as the other particles in the formulation. Therefore, milling in such cases may actually result in particle size growth rather than reduction.

One key aspect of ISET's successful particle deposition method is the ink formulation. ISET's precursor materials are in the form of nano particle powders and they can be put into ink and/or paste form and deposited successfully onto glass/Mo substrates in the form of thin layers. Using this low cost approach ISET has already demonstrated CIS solar cells with 12.4% efficiency.

2.2 Specific goals of the present program

Higher bandgap chalcopyrite absorbers are more attractive for PV applications than CIS because they offer the possibility of higher conversion efficiencies and higher voltages. It has also been discovered that addition of Ga and S into the absorber layers improve the overall process yield in terms of device efficiencies as well as film adhesion. Therefore, the specific goal of this Phase I project was the fabrication of large bandgap or graded bandgap absorbers for higher efficiency devices. Additional tasks were designed to address the issues encountered in the monolithic integration of modules, specifically the issue of poor CIS layer nucleation within the Mo scribes on the bare glass surface. For sulfur inclusion studies an approach was adopted which involved sulfurization of selenized layers. First CIS films grown by the selenization of e-beam evaporated precursors were used for investigating and understanding the sulfurization method. Then the findings were applied to the films prepared by the non-vacuum technique.

3.0 Technical Results and Discussion

3.1 Sulfur diffusion studies

A high bandgap surface region can be formed on a CIGS absorber by sulfurization. Graded absorber structures with S-rich surface and Ga-rich contact regions have been grown and high efficiency solar cells have been fabricated on such graded absorbers [1]. Additional work describing S introduction into CIGS absorber layers by annealing these films in a H_2S atmosphere has also been published [2,3,4].

The purpose of this task was a systematic investigation of S distribution in absorbers which were subjected to a sulfurization step in H_2S gas at an elevated temperature. The study was carried out on films with various Cu/In and Ga/(Ga+In) ratios to determine if changes in the original film composition would influence the resulting S concentration profiles.

CIS and CIGS films were grown by a two-stage selenization method. Cu-In and Cu-In-Ga metallic precursors were first deposited on glass/Mo substrates by the e-beam evaporation technique and then they were selenized in a 5% H_2Se + 95% N_2 atmosphere at around

450 °C to form the selenides. CIS films with Cu/In stoichiometric ratios varying from about 1.1 to 0.8 were obtained. Compositional variation was achieved by varying the thicknesses of the evaporated Cu, In and Ga layers. film thicknesses were controlled using a crystal oscillator head mounted in the e-beam evaporation system. For the CIGS layers, the overall Cu/(Ga+In) ratio was fixed at 0.95 and the Ga/(Ga+In) ratio was varied by increasing the Ga content of the metallic precursor films. After selenization, the absorber layer thicknesses were measured by a TENCOR profilometer and they were in the 2.0-2.5 μm range. The sample numbers and the information about the original selenide samples are given in Table 1.

Table 1 The CIS and CIGS samples used in the sulfurization studies.

Sample Number	**Cu/In ratio**	**Cu/(In+Ga) ratio**	**Ga/(Ga+In) ratio**
1973A	1.1		
1973B	1.0		
1973E	0.86		
1975A		0.95	0.1
1976A		0.95	0.25
1977A		0.95	0.4

The CIS and CIGS layers of Table 1 were subjected to a 10% H_2S+ 90% N_2 atmosphere at 575 °C for 20 minutes for sulfurization. Auger depth profiles were obtained to determine S distribution in the sulfurized layers. Scanning electron micrographs were used to study the micro structure of the absorbers.

Figures 2a, 2b and 2c show a set of Auger depth profiles obtained from three sulfurized CIS films. As can be seen from this data there is a definite and strong relationship between the composition of the original CIS film and the distribution of S in the $CuIn(Se,S)_2$ (CISS) absorber formed as a result of the sulfurization step. Sulfur distribution is near uniform in the CISS film of Figure 2a, which was obtained by the sulfurization of the Cu-rich CIS sample No. 1973A of Table 1. Sulfur diffusion, on the other hand, was greatly curtailed in the stoichiometric sample 1973B and the In-rich sample 1973E. As shown in Figure 2b, sulfurization of the stoichiometric CIS film gave a S profile with most of the S near the surface region. In this case there is little S deep in the bulk of the absorber. For the highly In-rich sample of 1973E however, a large peak of S is observed near the Mo/absorber interface in addition to the S peak near the surface of the absorber (Figure 2c). The (S+Se) concentrations in all of the profiles of Figure 2 are relatively flat, indicating that S has replaced Se in regions where it could penetrate.

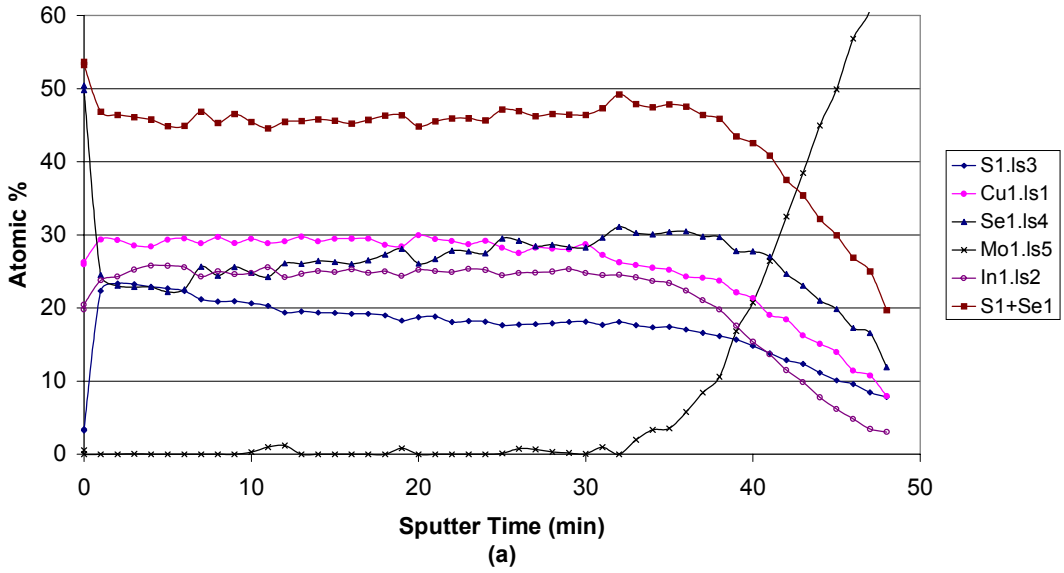

Figure 2a Auger depth profile taken from sample 1973A after sulfurization at 575 °C for 20 minutes

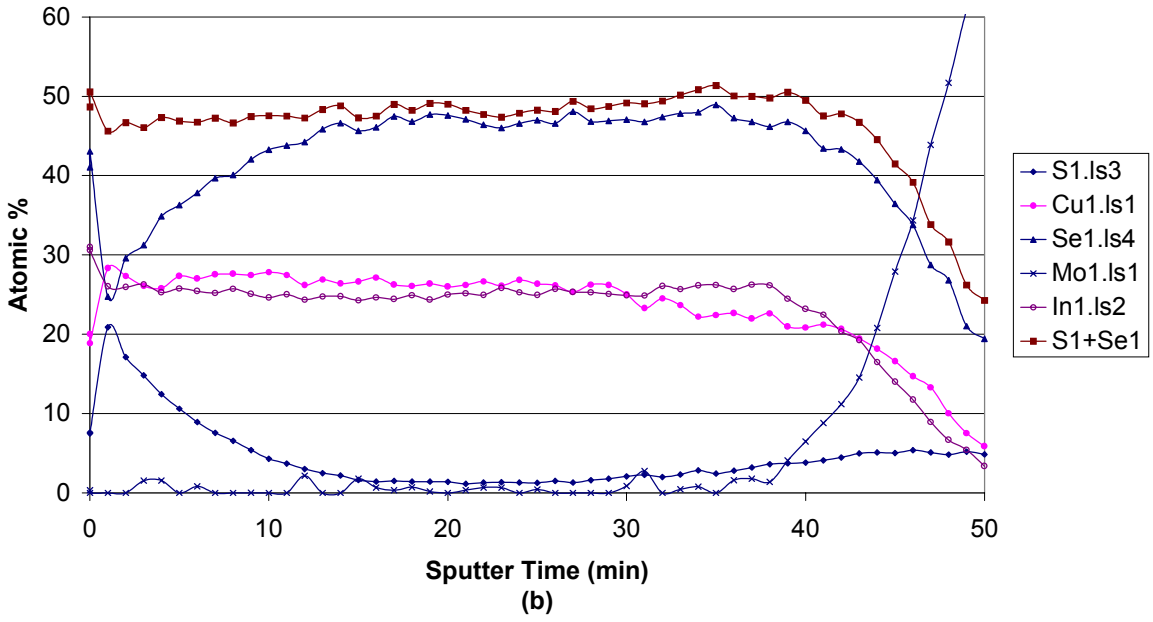

Figure 2b Auger depth profile taken from sample 1973B after sulfurization at 575 °C for 20 minutes.

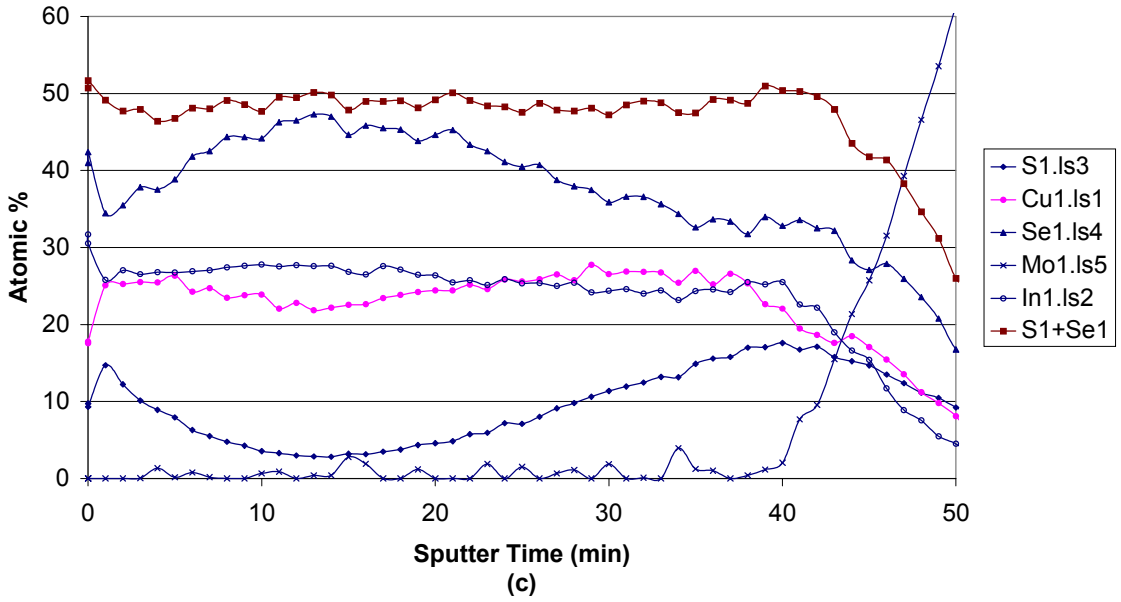

Figure 2c Auger depth profile taken from sample 1973E after sulfurizaiton at 575 °C for 20 minutes

What could be the reason for the large difference observed between the S profiles of Figures 2a 2b? Sample 1973A before sulfurization was a Cu-rich CIS film with Cu/In ratio of 1.1. Therefore, this film contained a secondary phase of Cu_2Se.
Using the Cu/In ratio of 1.1, one can estimate that Se which is chemically tied to the Cu_2Se secondary phase in this sample constituted about 2.4 atomic percent of the total Se content. Therefore, an argument based on possible replacement of Se with S within the excess Cu_2Se phase during the sulfurization step could not explain the approximately 20 atomic percent S observed in the sulfurized layer. One possible explanation for the promotion of S inclusion in the Cu-rich CIS layer can be the existence of a liquid phase of Cu-(Se,S) in such films at the high sulfurization temperature of 575 °C. It is plausible that kinetics of S inclusion is greatly accelerated by the presence of such a liquid phase.

The microstructure of CIS layers grown by the selenization technique is known to be strongly dependent on the Cu/In ratio. Cu-rich layers typically have large columnar grains. Grain size in In-rich material is smaller especially near the Mo interface. The cross sectional SEM of Figure 3a shows the microstructure of sample 1973A after the sulfurization step. Grains that are larger than 2 μm in size can be seen in this Cu-rich material which is well crystallized and dense. It should be noted that comparison of the cross sectional SEMs of absorber films before and after the sulfurization step indicated that the film micro structure was formed and fixed during the selenization process and did not change further during the sulfurization treatment at 575 °C.

There have been several reports in the literature on the S distribution profiles in sulfurized CIGS layers. The Auger depth profile given in reference [1], for example, showed high S concentration near the surface and contact regions of an absorber layer, which was used for the fabrication of a 15% efficient solar cell. The details of the process employed for the growth of this absorber, however, was not described. Nakada et al.[3], upon their investigation of the sulfurization of co-evaporated CIGS layers, reported S profiles that were very similar to the one depicted in Figure 2b. In that study the starting CIGS absorbers reportedly had large grains and they were near-stoichiometric, just as our sample 1973B.

The S distribution of Figure 2b is an example of a typical diffusion profile with most of the S residing near the surface of the sulfurized absorber. However, the profile of Figure 2c has an additional S "hump" near the Mo/absorber interface. This behavior can be explained by the micro structural differences between the films of Figures 2b and 2c.

It is known that the grain size distribution through the thickness of a CIS film grown by the two-stage selenization technique is non-uniform especially if the film is highly In-rich. The typical micro structure of such In-rich layers displays relatively large grains near the surface region and much smaller grains near the Mo/absorber interface. If S diffuses fast along the grain boundaries and then moves more slowly into the bulk of the grains, the small grain region near the back contact of In-rich films is expected to accommodate more sulfur than the larger grain near-surface region. This, in turn, would give rise to the "U-shaped" S profile of Figure 2c. The cross sectional SEMs of the samples 1973B and 1973E shown in Figures 3b and 3c support this argument. The grains in sample 1973E are smaller than those in the well crystallized sample of 1973B, especially near the Mo contact. It should be noted that although the SEMs of Figure 3 belong to sulfurized layers, they also represent the typical micro structures of the
original CIS absorbers as stated earlier.

Nakada et al. had previously reported the effect of microstructure on the S diffusion profiles in sulfurized CIGS films [3]. In that study, the growth temperature of the CIGS absorber was reduced from the standard 550 °C to 370°C to obtain a uniformly small-grained film, which was then sulfurized. Sulfur content in the small-grained absorber was uniformly higher than that found in the standard large-grained film. In our samples with graded grain size, the S profile is also graded giving rise to the observed double "hump" behavior. It should be noted that this micro structure-based argument may only be valid for the near-stoichiometric and Cu-poor absorbers. For the Cu-rich films such as sample 1973A, the S diffusion mechanism must be drastically different because we would not expect to observe much S diffusion into the large grain material of Figure 3a if the above micro structure argument were singly invoked.

A model was recently offered to explain the mechanism of S diffusion into CIS layers by exposing the CIS surface to S vapors or H_2S gas [5]. According to this model, first a surface reaction which is kinetically controlled occurs between the CIS surface and the

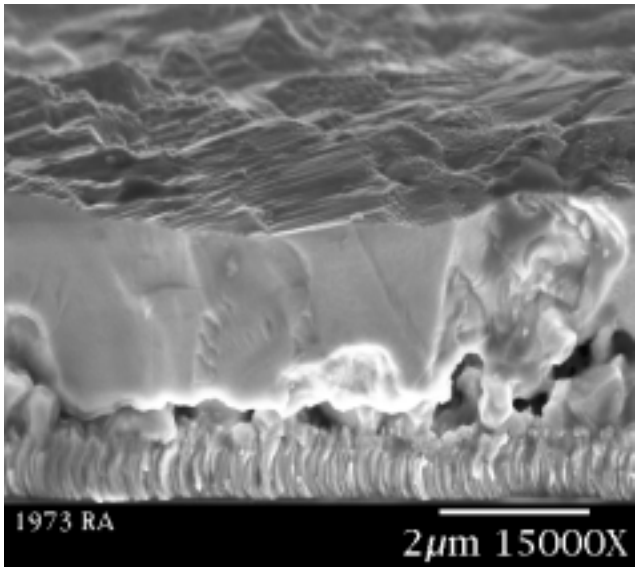

CIS (a)

Mo

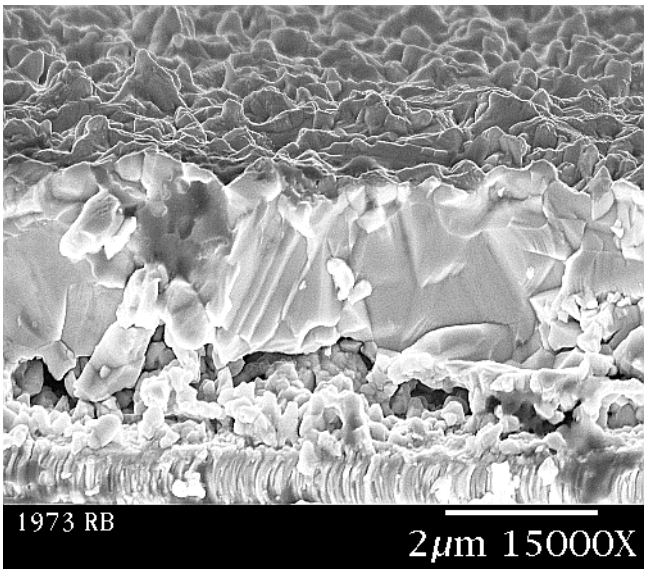

(b)

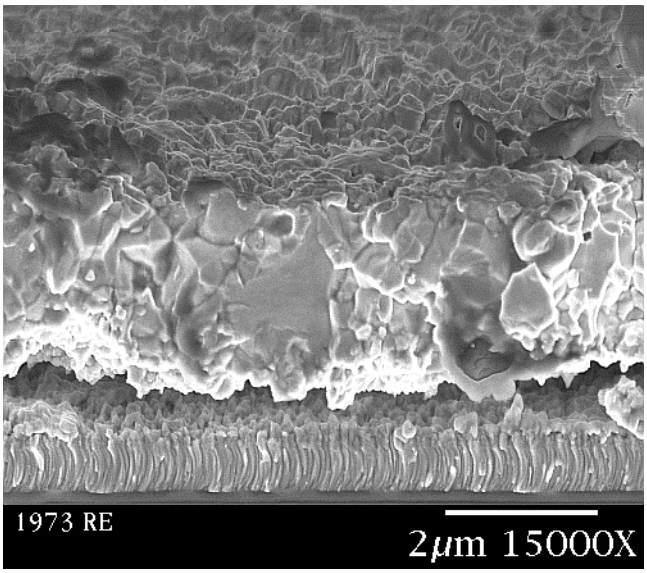

(c)

Figure 3

SEMs of cleaved samples a) 1973A, b)1973B and c)1973E after the sulfurization step, taken at 80° tilt to show both the cross section and the film surface .

S source, forming a thin $CuInS_2$ layer. This is followed by an interdiffusion process between the $CuInS_2$ and the $CuInSe_2$ layers. Using this model and experimental data, M. Engelmann and R. Birkmire recently derived a bulk diffusion constant of sulfur in slightly Cu-rich CIS layers to be $D=1.5x10^{-12}$ cm^2/sec at 475 °C. For a 20-minute sulfurization time at 475 °C, the S profile is expected to extend into the absorber layer by about $(Dt)^{½}$ or 0.4 μm. In our experiments we employed a sulfurization temperature of 575 °C. Extrapolating the previous data, the diffusion constant and $(Dt)^{½}$ were calculated to be about 10^{-10} cm^2/sec and 3.4 μm, respectively at 575 °C. Therefore, S would be expected to penetrate the whole thickness of the CIS absorber under these sulfurization conditions as we have observed for the Cu-rich film of 1973A.

The S profiles of the present work given in Figures 2b and 2c suggest that the S diffusion constant in a near-stoichiometric or Cu-poor CIS absorber is at least two orders of magnitude lower than the value previously reported in the literature. Therefore, the S diffusion mechanism in CIS-type materials is a very strong function of the original stoichiometry of the absorber. As stated before, the enhanced S distribution in Cu-rich CIS may be due to the existence of a liquid phase. There is, however, also the possibility of the influence of intrinsic defects which are expected to be very different in Cu-rich and In-rich CIS films. The exact nature of the S diffusion mechanisms in Cu-rich and In-rich CIS layers is currently under investigation. Time and temperature dependent studies of S profiles are being carried out to calculate the S diffusion constants in absorbers with various compositions.

The Auger depth profiles of sulfurized CIGS films are shown in Figure 4. As expected, the Ga concentration is graded in these layers, with most of the Ga residing near the Mo/absorber interface. Although the overall Cu/(Ga+In) ratio was fixed at 0.95 for all three layers of Figure 4, the S concentration profile still displayed the double "hump" behavior. Furthermore, S peak near the Mo interface got larger as the Ga concentration in the film increased (Figure 4c). We found no correlation between the Ga and S concentrations, i.e. S/Ga ratio was not a constant, indicating that there was not a preferred chemical reaction between these two species. Therefore, once again, the segregation of S into Ga-rich regions of the absorber layers was explained by the varying micro structure within these absorbers. It is known that addition of Ga into CIS reduces the grain size. Since most of the Ga in selenized CIGS layers resides in the back, the grain size is expected to be the smallest near the Mo interface of the most Ga-rich sample (1977A). This trend was observed and confirmed by the examination of the cross sectional SEMs taken from the samples of Figures 4a, 4b and 4c.

3.2 Device measurements

The above study demonstrated that S distribution in absorbers obtained by the sulfurization technique was a strong function of the overall stoichiometry of the original CIS layer and it also depended on the Ga content of the graded CIGS films. To study the correlation between the S and Ga distributions and the device behavior, we carried out another set of experiments that involved varying the composition of the Ga containing absorbers. Devices were fabricated on CIGS and CIGSS absorbers depositing CBD CdS layers and ZnO contacts. Cell measurements were carried out at CSU at Prof. J. Sites' laboratory.

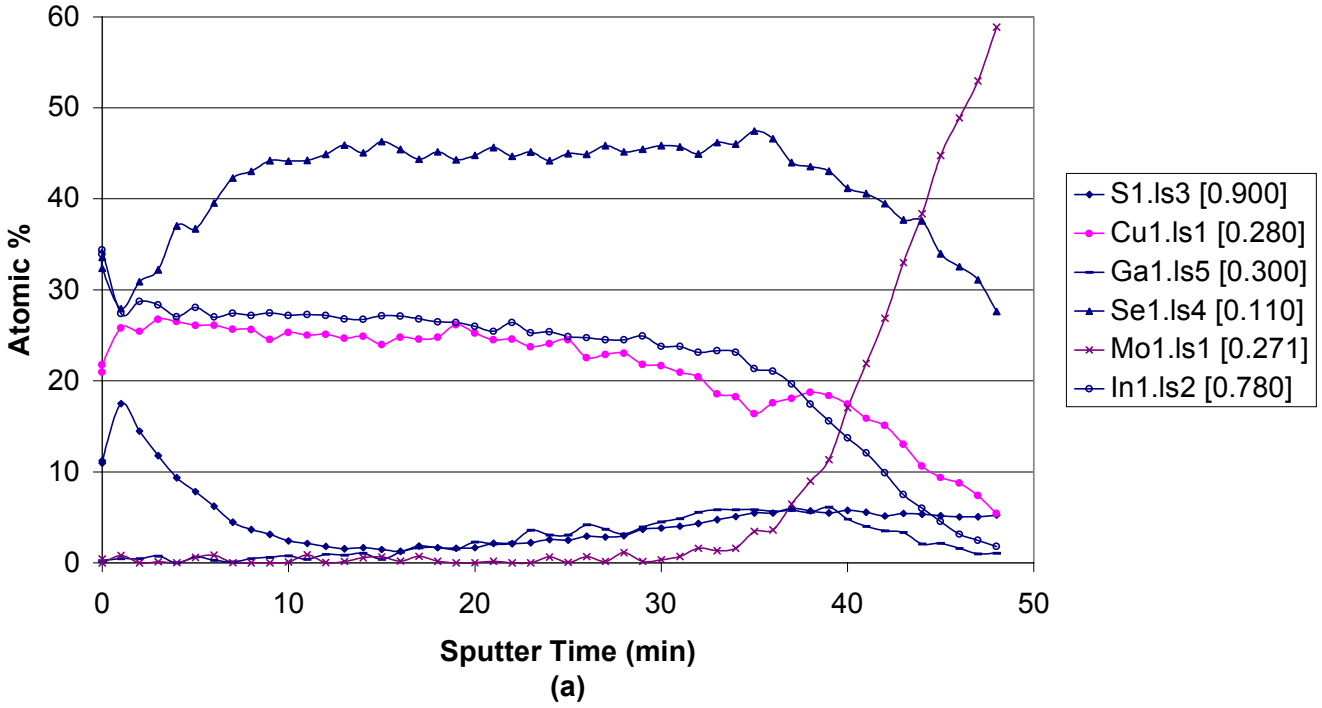

Figure 4a Auger depth profile taken from sample 1975A after sulfurization at 575 °C for 20 minutes.

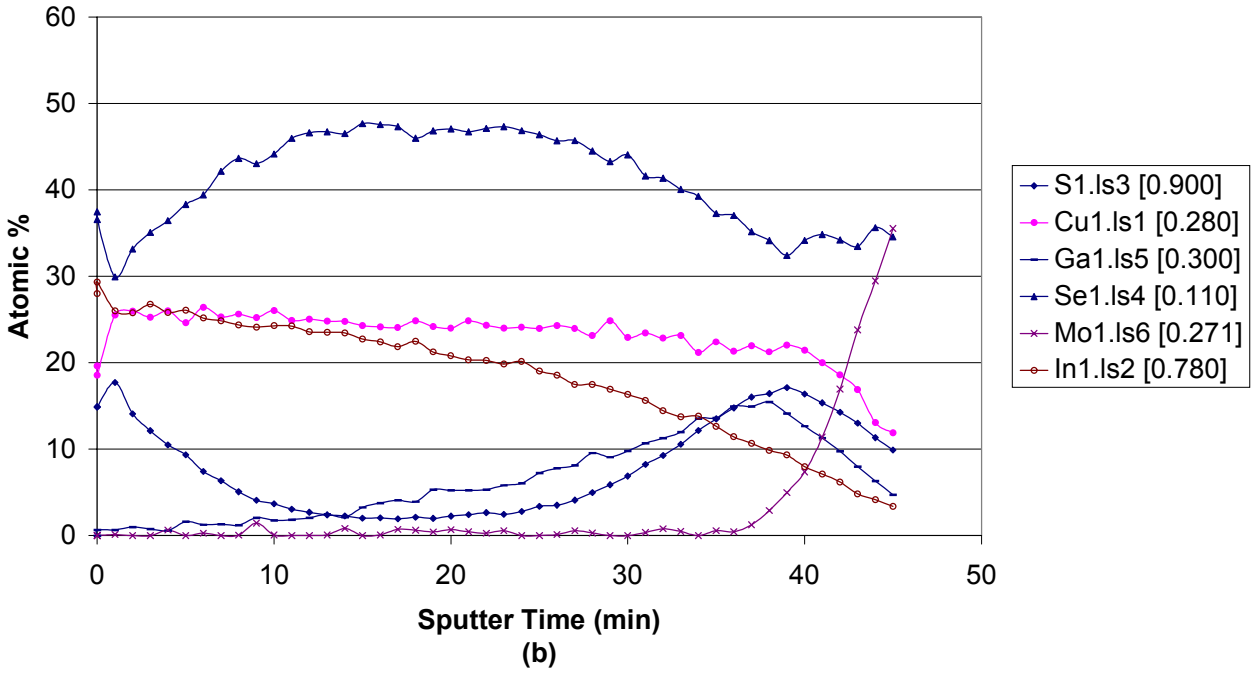

Figure 4b Auger depth profile taken from sample 1976A after sulfurization at 575 °C for 20 minutes.

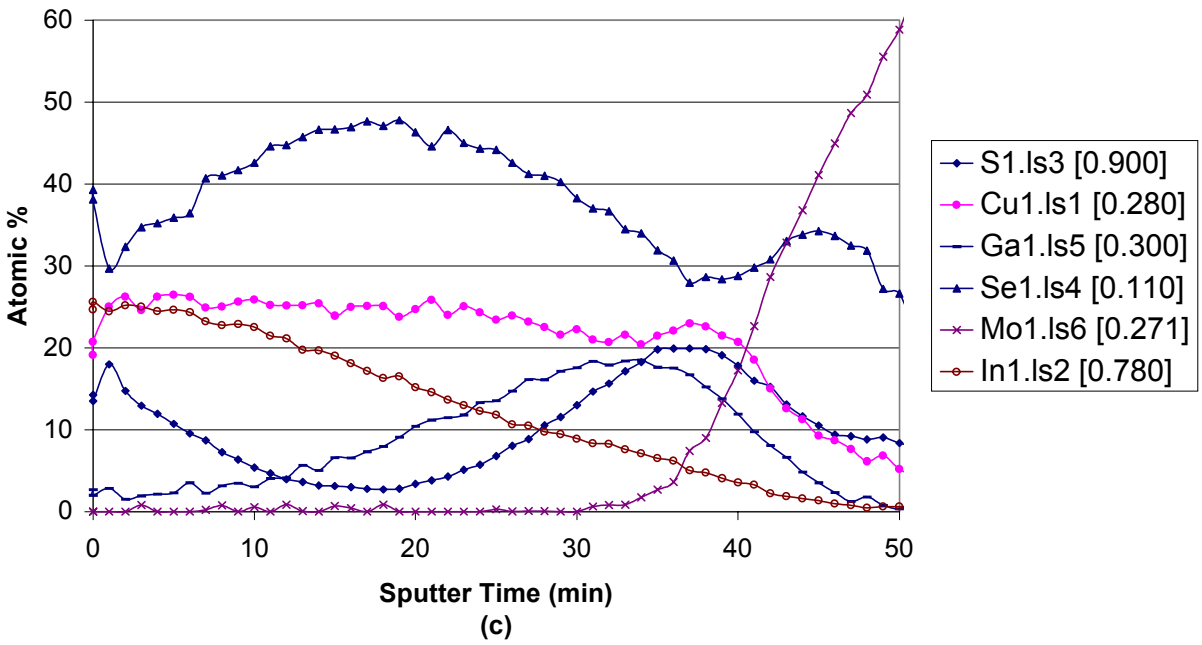

Figure 4c Auger depth profile taken from sample 1977A after sulfurization at 575 °C for 20 minutes

Table 2 contains the information about the nature of the absorber layers used, the solar cell parameters of the devices fabricated on these absorber layers, and the effective bandgap values of the absorbers deduced from the long wavelength region of the quantum efficiency data.

Table 2 Solar cell parameters for 0.1 cm^2 devices fabricated on near stoichiometric (A,B) and Cu-poor (C,D) CIGS and CIGSS absorbers. **A** is the diode factor, **R** is series resistance and **r** is shunt resistance. $\mathbf{E_g}$ is the effective minimum bandgap derived from the QE data.

Sample

No	Description	J_{sc}	V_{oc}	FF	Eff	A	R	r	E_g
	Near-stoichiometric								
A	CIGS	38.4	488	67.4	12.6	2.0	0.2	950	1.08
B	CIGSS (after S)	36.8	559	66.5	13.7	2.0	1.0	1500	1.09
	Cu-poor								
C	CIGS	28	574	67.8	10.9	2.0	0.4	1000	1.17
D	CIGSS	25	608	61.4	9.3	2.5	0.05	300	1.28

The Ga/(Ga+In) ratio in all of the samples of Table 2 was fixed at 0.40. The near stoichiometric samples A and B had a Cu/(Ga+In) ratio of about 0.95. The Cu/(Ga+In) ratio for the Cu-poor samples C and D was around 0.80. After the selenization step the CIGS absorbers were annealed at 575 °C in nitrogen for 20 minutes. For the case of CIGSS layers this annealing step was carried out in a 10% H_2S atmosphere at the same temperature for the same period of time. Auger depth profiles for the two CIGSS films of Table 2 are given in Figures 5a and 5b.

One can make the following observations comparing the Auger data of Figures 5a and 5b: i) For the same fixed Ga/(Ga+In) ratio, Ga in the Cu-poor absorber layer has diffused more to the surface of the film as a result of the high temperature annealing step, ii) although the surface concentration of S is similar in both layers, the concentration level in the bulk is higher in the Cu-poor absorber, iii) there is a S peak near the Mo interface in both the near-stoichiometric and Cu-poor layers.

Observations ii) and iii) are in agreement with the results of the S diffusion studies reported in the previous sub-section. The S peak near the Mo interface is due to the small grain size of the material near that interface and since both of the films of the present study contained high levels of Ga near the Mo contact, a large S peak is expected in that region of the film irrespective of the overall Cu/(Ga+In) ratio. Similarly, the Cu-poor film with smaller overall grain size is expected to accommodate more S in its bulk as is the case in Figure 5b. Observation i) is a new finding which suggests that Ga diffusion in graded CIGS layers grown by selenization is a function of the overall stoichiometry. This topic is now under further investigation by the ISET team.

Using the S and Ga distribution profiles of Figures 5a and 5b one can estimate the minimum bandgap values of these graded absorbers. We made these calcualtions and found the expected bandgap value to be in the range of 1.05-1.1 eV for sample B and 1.2-1.25 eV for sample D. These values are in good agreement with the values deducted from the quantum efficiency data as shown in Table 2.

The device data in Table 2 and the Auger profiles of Figure 5 suggest that the effect of the sulfurization step on the stoichiometric CIGS absorber layer was the introduction of a S-rich surface region on this film which improved the open circuit voltage of the fabricated solar cell without appreciably affecting the effective bandgap of the bulk of the absorber. The J_{sc} value of the solar cell fabricated on the sulfurized absorber was somewhat lower than the one made on the original CIGS layer. However, the difference was only 1.6 mA/cm^2. The short circuit current density dropped precipitously in the cell fabricated on the Cu-poor CIGS absorber and declined even further in the device fabricated on the sulfurized Cu-poor absorber. The rise of the effective bandgap from 1.08 eV in sample A to 1.17 eV in sample C can be explained by the extensive Ga diffusion observed in sample C. The E_g increase from 1.17 eV (sample C) to 1.28 eV (sample D) can also be explained by S inclusion in the bulk of sample D (see Figure 5b). However, these bandgap increases are not sufficient to explain the large drop observed in the J_{sc} values of the devices fabricated on Cu-poor absorbers. Figure 6 shows the relative QE data obtained at CSU from the devices fabricated on samples B and D. It is clear that, in addition to the obvious differences in the long wavelength cut-offs in these devices, there is also a long wavelength loss in sample D

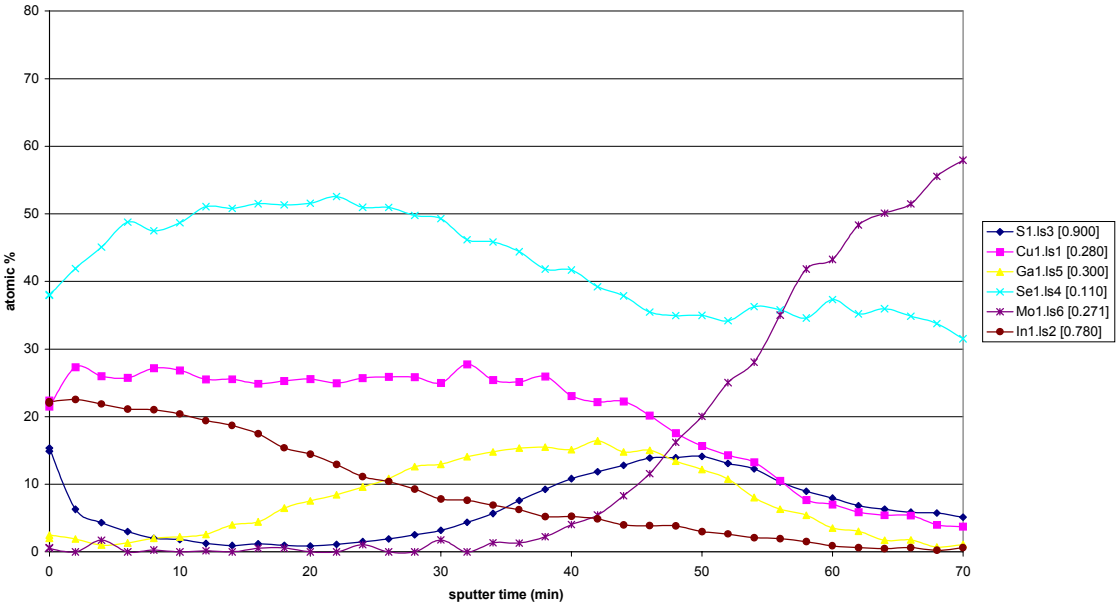

Figure 5a Auger depth profile taken from sample B of Table 2.

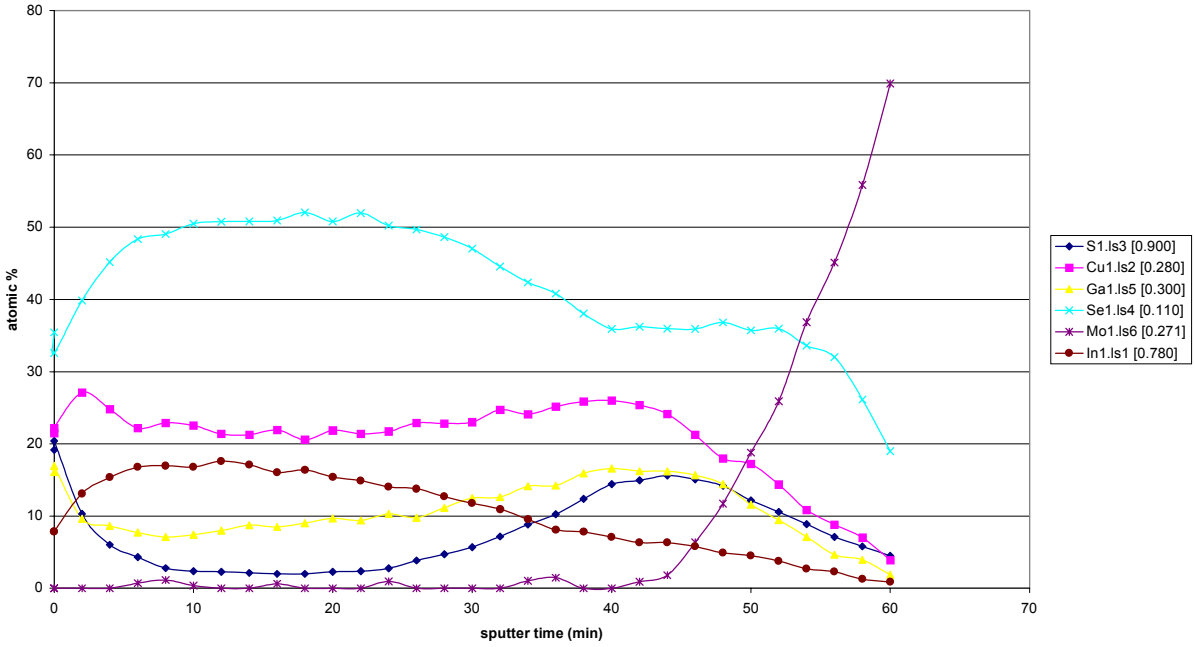

Figure 5b Auger depth profile of sample D of Table 2.

which can be due to poor carrier collection in the high-Ga(S) containing absorber. Capacitance measurements made on the samples of Table 2 showed little difference between cells, indicating a fairly consistent hole density value of about $2x10^{16}$ cm^{-3}, with an apparent increase within 0.2 μm of the junction.

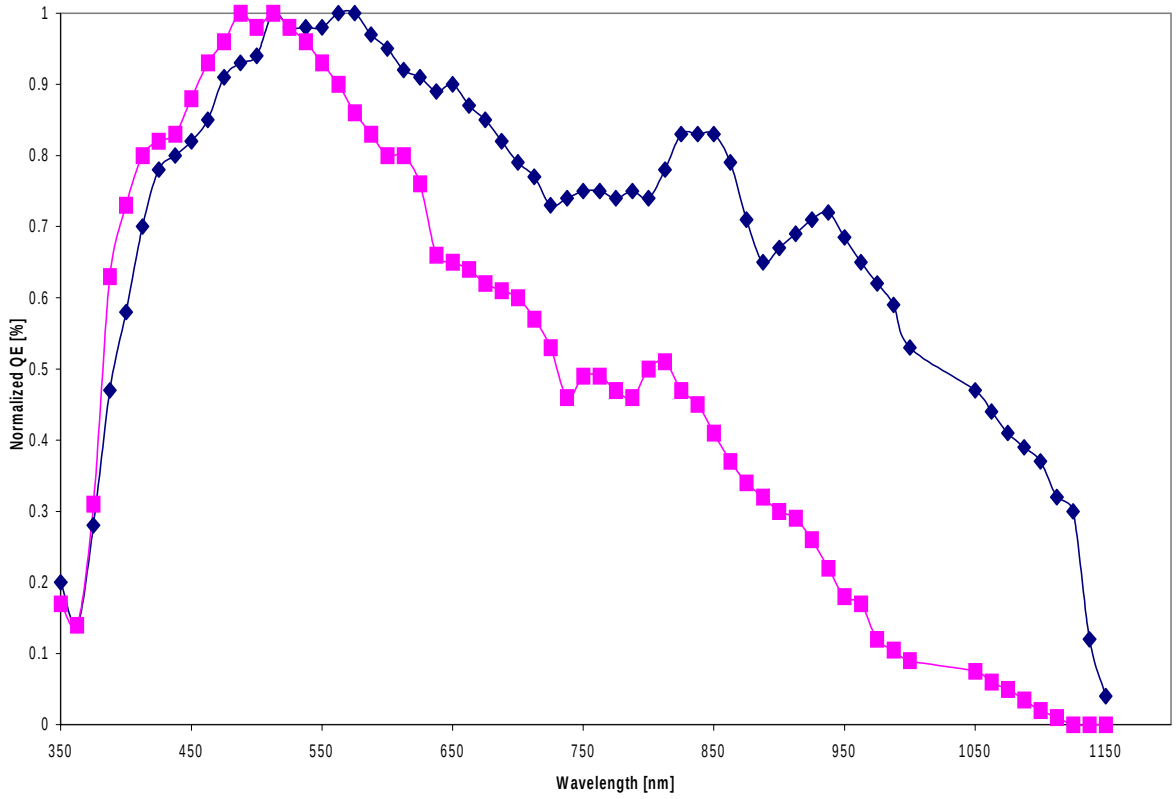

Figure 6. Quantum efficiency data (relative) for devices made on sample B (♦) and D (■) of Table 2.

The analysis and results presented in this section of the report clearly demonstrated that the overall stoichiometry and the micro structure of the CIS and CIGS layers influence the eventual distribution of Ga and S in absorbers grown by the two-stage selenization/sulfurization techniques. These findings were then applied to the processing of a CIGSS layer, which was grown by the non-vacuum approach. An absorber which was Ga-rich near the Mo contact and S-rich near the surface was prepared. Solar cells were fabricated on this absorber with conversion efficiencies of about 10% with V_{oc}=0.51 V, J_{sc}= 33 mA/cm^2 and FF= 61%.

3.3 Mini-modules

Development of monolithically integrated mini-modules employing CIS absorbers grown by the non-vacuum technique was another important task of this Phase I program. Monolithic integration techniques commonly used in vacuum-based CIS technologies are not necessarily directly applicable to the non-vacuum process. One major problem arises if the films do not nucleate properly on the bare glass surfaces, which get exposed when Mo is scribed by laser, forming parallel and isolated Mo pads. If the portion of the CIS film deposited on the scribed region is discontinuous and if the coverage by the CIS at the edges of the Mo pads is not good, shunting paths may result between the adjacent Mo pads as well as between the ZnO and Mo contacts of the individual cells within the module structure. During this research period we carried out work on both improving the CIS film nucleation between the Mo pads and optimizing the laser scribing process for Mo and Mo/CIS layers.

The SEM of Figure 7 shows a typical scribe performed on a Mo/CIS structure using an infrared YAG laser beam. Although the details change with laser power, rep rate and the scribing speed it is common to observe a melted region along the two edges of the scribed

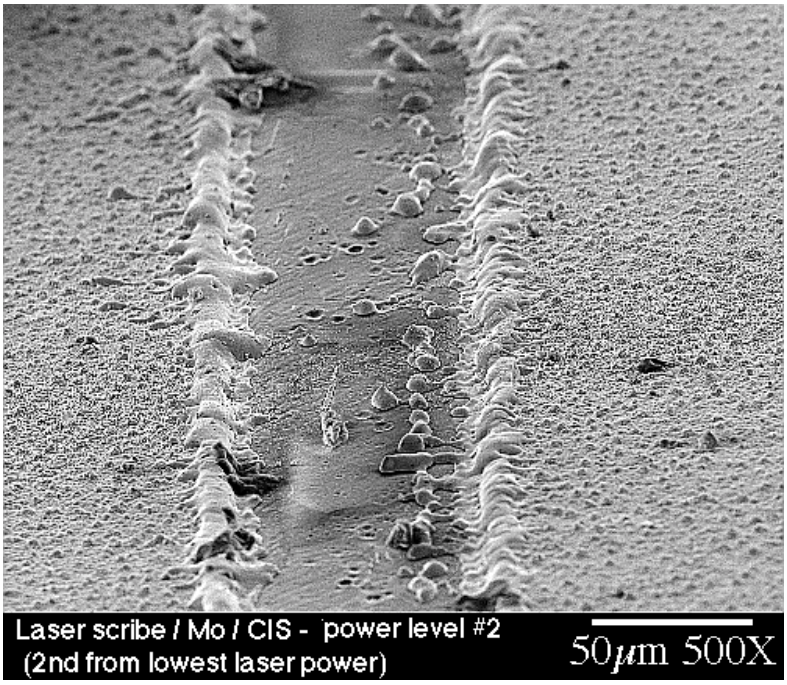

Figure 7 Line scribed into a Mo/CIS structure by a YAG laser beam. The region in the middle is the exposed glass surface.

line as is the case in Figure 7. Microprobe measurements made on these melted regions indicated that they were Cu-rich. Apparently, upon heating by the laser, the CIS in these

regions melt and the high vapor pressure In-Se species evaporate leaving behind a low resistivity Cu-rich area. Similarly, when a Mo layer is scribed it is common to observe melted Mo regions along the scribed line.

During this research period we addressed both of these issues and optimized the laser scribing technique to minimize the melted regions along the scribed lines. The typical width of the scribes we could obtain is presently 15-25 μm and there are few debris along the scribe lines. Under the newly developed conditions we are working, the Mo layer is not melted extensively by the laser beam, and therefore, we do not have the Mo mounds which we often observed in the past along the edges of the scribed lines. After carrying out the above mentioned tests at an outside laboratory, ISET is now in the process of setting up the laser scribing capability for 1 ft^2 size modules in-house.

Figures 8 and 9 show the illuminated I-V characteristics and the quantum efficiencies of two mini-modules fabricated at ISET using the non-vacuum particle deposition technique. The 134.4 cm^2 device (Figure 8) utilized a CIS absorber layer and it was obtained by parallel connection of two mini-modules, approximately 65 cm^2 area each. This mini-module consisted of 16 cells in series and its efficiency was measured to be 6.28%.

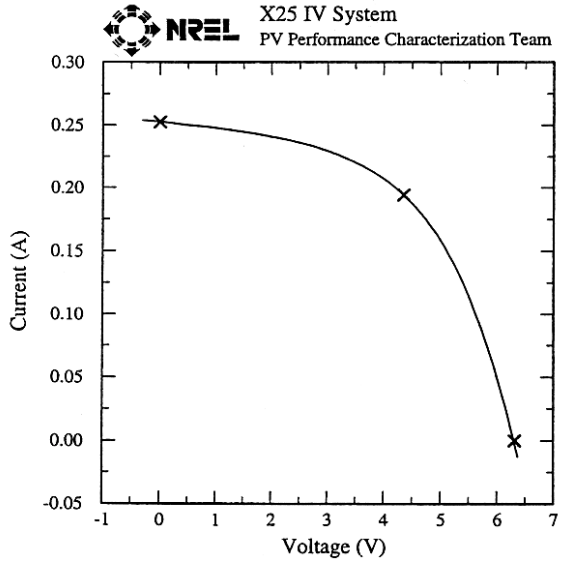

V_{oc} = 6.312 V
I_{sc} = 0.2526 A
J_{sc} = 1.879 mA/cm^2
Fill Factor = 52.97 %

I_{max} = 194.3 mA
V_{max} = 4.347 V
P_{max} = 844.6 mW
Efficiency = 6.28 %

After 10 minute soak at P_{max}., 2 minute cool.
Aperture area.

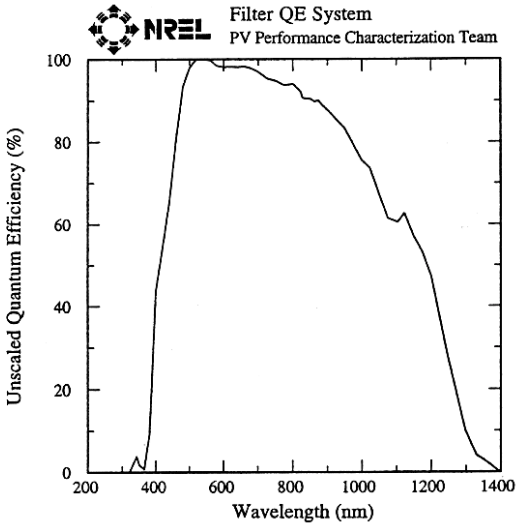

Voltage Bias: 0.0 V
Light bias for 22.4 mA
Light Bias region area: 134.4 cm^2
Light Bias Density: 0.1665 mA/cm^2

Aperture area.

J_{sc} Estimate:
J_{sc} (Global) = 40.3 mA/cm^2

Figure 8 Illuminated I-V characteristics and the quantum efficiency data of a 134.4 cm^2 area mini-module fabricated on CIS absorbers grown by the non-vacuum technique.

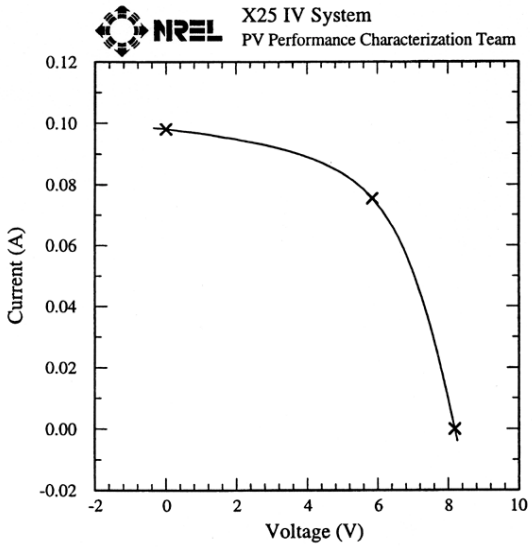

V_{oc} = 8.187 V
I_{sc} = 0.09807 A
J_{sc} = 1.543 mA/cm^2
Fill Factor = 54.94 %

I_{max} = 75.46 mA
V_{max} = 5.846 V
P_{max} = 441.1 mW
Efficiency = 6.94 %

After 10 minute soak at P_{max}., 2 minute cool.
Taped by ISET, Aperture area.

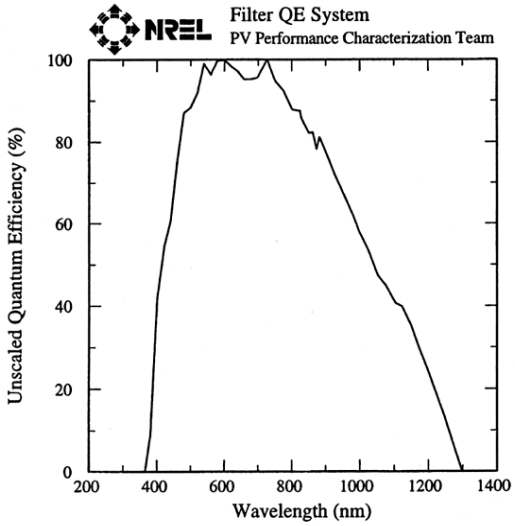

Voltage Bias: 0.0 V
Light bias for 0.0376 mA
Light Bias region area: 1.000 cm^2
Light Bias Density: 0.03756 mA/cm^2

Aperture area, Area approximate.
Taped by ISET

J_{sc} Estimate:
J_{sc} (Global) = 35.9 mA/cm^2

Figure 9 Illuminated I-V characteristics and the quantum efficiency data of a 63.57 cm^2 area mini-module fabricated on a CISS absorber grown by the non-vacuum technique.

The 63.57 cm^2 device of Figure 9 was fabricated using a graded CISS absorber with a S-rich surface. It had 17 cells in series. The average individual cell voltage in this module was 481mV compared to 395 mV for the module of Figure 8. The efficiency was measured to be 6.94%. The quantum efficiency data indicates poor collection at long wavelengths compared to the pure CIS absorber of Figure 8. There is little difference in the short wavelength responses of the CIS and CISS mini-modules.

4.0 Future work

During this Phase I program, work was concentrated on three major tasks; i) S diffusion in CIS films was studied and using this understanding, a process was developed that, for the first time, yielded graded CISS absorbers using ISET's non-vacuum deposition technique, ii) a module integration approach was developed that led to the demonstration of about 7% efficient modules using the larger bandgap absorber, iii) a back contact structure was developed that eliminated mechanical peeling problems and improved yields. The future work will now concentrate on further efficiency and yield improvements, stability studies and alternate buffer layers.

Sulfur diffusion studies need to be completed. With careful time/temperature dependent diffusion studies it should be possible to develop an understanding of the mechanisms that dominate the diffusion of S in Cu-rich and Cu-poor CIS layers. Having established a baseline process that can provide mini-modules by the non-vacuum process, ISET now is in a position to initiate work on module lamination, stability studies and investigation of possible transient effects. This task will constitute an important portion of the Phase II program. Identification and understanding of the possible loss mechanisms or transient effects due to lamination and/or long term light exposure will be important for this new low-cost, non-vacuum CIS technology. Work on module integration will have to continue to reduce the losses in the existing module structures. All of the necessary components of a laser scriber system has been acquired by ISET and this system will be operational during the early months of the Phase II program. Efforts to eliminate the CdS buffer layer will include investigation of various sulfides and selenides that can be deposited on the absorbers through non-vacuum techniques. During the Phase I program, we adapted a typical mini-module size of 3"x4" to carry out the research work. During the Phase II program this size will be increased to 6.5"x6.5", while the processing capability of our reactors and the module integration equipment will be 13"x13".

5.0 Acknowledgments

Authors acknowledge the contributions of ISET team members University of Florida (T. Anderson), IEC (R. Birkmire), NREL (R. Noufi, H. Ullal) and CSU (J. Sites, J. Hiltner). Auger measurements by A. Swartzlander and SEM work by R. Matson of NREL are gratefully acknowledged.

6.0 References

1. Tarrant D, Ermer J. I-III-VI_2 multinary solar cells based on $CuInSe_2$. *Proceedings 23rd IEEE Photovoltaic Specialists Conference* 1993; 372-378.
2. Kushiya K, Kuriyagawa S, Kase T, Tachiyuki M, Sugiyama I, Satoh Y, Satoh M, Takeshita H. The role of $Cu(InGa)(SeS)_2$ surface layer on a graded band-gap $Cu(InGa)Se_2$ thin-film solar cell prepared by two-stage method. *Proceedings 25th IEEE Photovoltaic Specialists Conference*1996; 989-992.
3. Nakada T, Ohbo H, Watanabe T, Nakazawa H, Matsui M, Kunioka A. Improved $Cu(In,Ga)(S,Se)_2$ thin film solar cells by surface sulfurization. *Solar Energy Materials and Solar Cells* 1997; **49**: 285-290.
4. Kushiya K, Tachiyuki M, Kase T, Nagoya Y, Sugiyama I, Yamase O, Takeshita H. Bandgap control of large-area $Cu(InGa)Se_2$ thin-film absorbers with Ga and S. *Proceedings 2nd World Conference on Photovoltaic Energy Conversion, Vienna, Austria* 1998; 424-427.
5. Birkmire R, Engelmann M. Chemical kinetics and equilibrium analysis of I-III-VI films. *Proceedings 15th NCPV Photovoltaic Review Conference, AIP Conf. Proc. 462* 1998; 23-28.

REPORT DOCUMENTATION PAGE

Form Approved
OMB NO. 0704-0188

1. AGENCY USE ONLY (Leave blank)	2. REPORT DATE	3. REPORT TYPE AND DATES COVERED
	August 1999	Phase I Annual Technical Report, 1 July 1998 – 30 June 1999

4. TITLE AND SUBTITLE
CIS-Type PV Device Fabrication by Novel Techniques; Phase I Annual Technical Report, 1 July 1998 – 30 June 1999

5. FUNDING NUMBERS
C: ZAK-8-17619-10
TA: PV905001

6. AUTHOR(S)
B.M. Basol, V.K. Kapur, C.R. Leidholm, A. Halani, G. Norsworthy, and R. Roe

7. PERFORMING ORGANIZATION NAME(S) AND ADDRESS(ES)
International Solar Electric Technology, Inc
8635 Aviation Blvd.
Inglewood, CA 90301

8. PERFORMING ORGANIZATION REPORT NUMBER

9. SPONSORING/MONITORING AGENCY NAME(S) AND ADDRESS(ES)
National Renewable Energy Laboratory
1617 Cole Blvd.
Golden, CO 80401-3393

10. SPONSORING/MONITORING AGENCY REPORT NUMBER
SR-520-26930

11. SUPPLEMENTARY NOTES
NREL Technical Monitor: H.S. Ullal

12a. DISTRIBUTION/AVAILABILITY STATEMENT
National Technical Information Service
U.S. Department of Commerce
5285 Port Royal Road
Springfield, VA 22161

12b. DISTRIBUTION CODE

13. ABSTRACT *(Maximum 200 words)*

This report describes work performed by International Solar Electric Technology, Inc. (ISET) during phase I of the R&D partnership subcontract titled "CIS-Type PV Device Fabrication by Novel Techniques." The objective of this program is to bring ISET's novel non-vacuum CIS technology closer to commercialization by concentrating on issues such as device-efficiency improvement, larger-bandgap absorber growth, and module fabrication. Advances made in CIS and related compound solar cell fabrication processes have clearly shown that these materials and device structures can yield power conversion efficiencies in the 15%-20% range. However, many of the laboratory results on CIS-type devices have been obtained using relatively high-cost vacuum-based deposition techniques. The present project was specifically geared toward developing a low-cost, non-vacuum "particle deposition" method for CIS-type absorber growth. There are four major processing steps in this technique: i) preparation of a starting powder containing all or some of the chemical species constituting CIS, ii) preparation of an ink using the starting powder, iii) deposition of the ink on a substrate in the form of a thin precursor layer, and iv) conversion of the precursor layer into a fused photovoltaic absorber through annealing steps. During this Phase I program, ISET worked on tasks that were geared toward the following goals: i) elimination of back-contact problems, ii) growth of large-bandgap absorbers, and iii) fabrication of mini-modules. As a result of the Phase I research, a Mo back-contact structure was developed that eliminated problems that resulted in poor mechanical integrity of the absorber layers. Sulfur inclusion into CIS films through high-temperature sulfurization in H_2S gas was also studied. It was determined that S diffusion was a strong function of the stoichiometry of the CIS layer. Sulfur was found to diffuse rapidly through the Cu-rich films, whereas the diffusion constant was at least three orders of magnitude smaller in Cu-poor layers. Additionally, S profiles in sulfurized CIS films were correlated with the distribution of the grain size through the film. Absorbers containing large concentrations of Ga near the Mo contact interface also had large S content in that same region due to the small grain size of the Ga-containing material. New work on monolithic integration procedures overcame the problem of low shunt resistance and yielded $CuIn(S,Se)_2$ (CISS) mini-modules of about 64-cm^2 area with close to 7% efficiency.

14. SUBJECT TERMS
photovoltaics ; CIS ; device fabrication ; "particle deposition" technique ; sulfur diffusion ; device measurements ; mini-modules ; non-vacuum ; back-contact ; device efficiency

15. NUMBER OF PAGES
26

16. PRICE CODE

17. SECURITY CLASSIFICATION OF REPORT	18. SECURITY CLASSIFICATION OF THIS PAGE	19. SECURITY CLASSIFICATION OF ABSTRACT	20. LIMITATION OF ABSTRACT
Unclassified	Unclassified	Unclassified	UL